THE JOURNAL OF PHYSICAL CHEMISTRY B

pubs.acs.org/JPCB Article

Stable Glasses of Organic Semiconductor Resist Crystallization

Kushal Bagchi, Marie E. Fiori, Camille Bishop, M. F. Toney, and M. D. Ediger*

Cite This: J. Phys. Chem. B 2021, 125, 461−466

Read Online

ACCESS | Metrics & More | Article Recommendations | Supporting Information

ABSTRACT: The instability of glassy solids poses a key limitation to their use in several technological applications. Well-packed organic glasses, prepared by physical vapor deposition (PVD), have drawn attention recently because they can exhibit significantly higher thermal and chemical stability than glasses prepared from more traditional routes. We show here that PVD glasses can also show enhanced resistance to crystallization. By controlling the deposition temperature, resistance toward crystallization can be enhanced by at least a factor of ten in PVD glasses of the model organic semiconductor Alq3 (tris(8-hydroxyquinolinato) aluminum). PVD glasses of Alq3 first transform into a supercooled liquid before crystallizing. By controlling the deposition temperature, we increase the glass → liquid transformation time thereby also increasing the overall time for crystallization. We thus demonstrate a new strategy to stabilize glasses of organic semiconductors against crystallization, which is a common failure mechanism in organic light emitting diode devices.

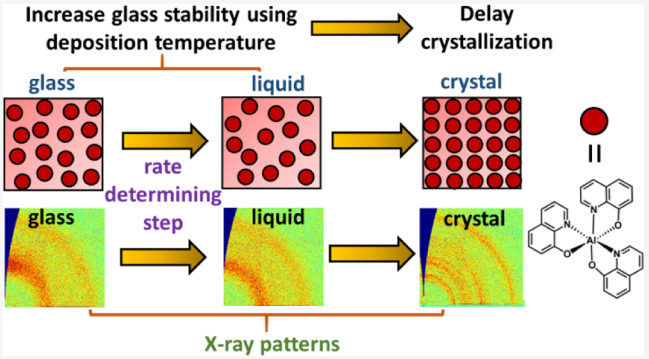

INTRODUCTION

Glasses are disordered and non-equilibrium solids that are traditionally formed by cooling a supercooled liquid.[1,2] Apart from being interesting from a fundamental physics perspective,[3] glassy solids are also used in a broad range of technological applications, from electrical transformers that use metallic glasses[4] to OLED (organic light emitting diode) devices that use molecular glasses.[5−7] While glasses offer several advantages over crystalline solids, such as macroscopic homogeneity (lack of grain boundaries) and compositional flexibility (dopants can be easily dispersed inside a glassy solid), a key limitation of glasses is their long-term stability.[8] Glasses physically age over time[9,10] and can crystallize.[11,12] Additionally, glasses can be more prone to chemical degradation than crystals.[8] The physical and chemical stability of molecular glasses has been shown to be vital to the device lifetime of OLEDs.[6,13]

Physical vapor deposition (PVD) can be used to form highly stable glasses.[14−16] This is significant technologically, as PVD is the standard route to prepare thin glassy films of organic semiconductors for OLED applications. The kinetic stability, as well as other properties of PVD glasses, is highly sensitive to the deposition temperature and rate.[17−19] The most stable PVD glasses are formed at a slow deposition rate and a deposition temperature that is 75−95% of the glass transition temperature. When annealed above the glass transition temperature, the most stable glasses formed by PVD can take up to ∼10^5 times longer to transform into a supercooled liquid than an ordinary liquid-cooled glass.[20] This enhanced kinetic stability in PVD glasses is often also accompanied by superior chemical stability. Relative to liquid-cooled glasses, stable PVD glasses have been shown to be more resistant to light-induced reactions,[21,22] reactions with atmospheric gases,[23] and water vapor uptake.[24] Depositing organic semiconductor layers (the emissive and electron transport layers) at temperatures that produce the most stable glasses was shown to increase the device lifetime of an OLED by a factor of five, relative to deposition at room temperature[6] (which resulted in a less stable glass).

While well-established strategies exist to increase the kinetic and chemical stability of PVD glasses, the same is not true for stability against crystallization. Preparing glasses that are stable with respect to crystallization is important for a broad range of applications. For instance, a common failure mechanism for OLED devices is crystallization of the glassy charge transport and emissive layers.[25,26] It has been shown that crystallization of the common electron transport layer Alq3 (tris(8-hydroxyquinolinato) aluminum) in OLEDs leads to cathode delamination, which in turn causes the formation of non-emissive dark spots.[26] For vapor-deposited organic glasses, there is only one example in the literature (to the best of our knowledge) where glass stability has been shown to influence crystallization kinetics; crystallization was shown to be ∼30%

Received: November 3, 2020
Revised: December 2, 2020
Published: December 24, 2020

https://dx.doi.org/10.1021/acs.jpcb.0c09925
J. Phys. Chem. B 2021, 125, 461−466

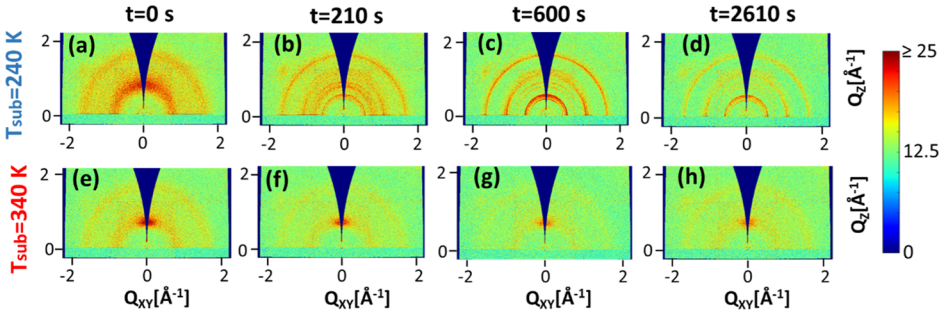

Figure 1. Two-dimensional X-ray scattering patterns for Alq3 glasses deposited at 240 (a–d) and 340 K (e–h) as a function of annealing time at 453 K, which is ≈5 K above the glass transition temperature of Alq3. While the glass deposited at 240 K shows sharp crystalline features by 210 s, the glass deposited at 340 K is largely amorphous after 2610 s of annealing.

slower in a stable PVD glass of celecoxib than for its liquid-cooled glass.[27] To test the generality and applicability of this result, crystallization studies need to be performed on a larger variety of glass formers, including organic semiconductors, and also across a broader range of conditions. Using glass stability to prevent or delay crystallization could have important implications for organic electronic devices such as OLEDs.

In this study, we investigate the role of deposition temperature on the crystallization of vapor-deposited glasses of Alq3, a molecule which has been used in OLED devices for several decades[28] and is also of interest for organic lasers[29] and spintronics.[30] We show that Alq3 glasses prepared at different deposition temperatures can vary by at least a factor of ten in crystallization time. We also show that crystallization of PVD glasses of Alq3 (upon annealing) follows a two-step process whereby the glass first transforms into a supercooled liquid and crystallizes thereafter. PVD glasses of Alq3 deposited at the optimal deposition temperature take longer to transform into a supercooled liquid and therefore also crystallize more slowly. Our study shows that like chemical and kinetic stability, the stability against crystallization in PVD glasses can also be modulated by at least an order of magnitude by controlling the substrate temperature during deposition.

METHODS

Sample Preparation. Alq3 (99.995% purity, trace metals basis) was purchased from Sigma-Aldrich and used without further purification. The films were deposited on ⟨100⟩ cut silicon wafer that had ∼2 nm of native oxide. PVD was performed in a vacuum chamber with a base pressure of $\sim 10^{-6}$ Torr. The films were deposited at a rate of 0.15–0.2 nm/s. The deposition rate was monitored during deposition with a quartz crystal microbalance. The films had a thickness of 450–600 nm. The film thickness was measured after deposition with variable angle spectroscopic ellipsometry.

GIWAXS. Grazing incidence wide angle X-ray scattering (GIWAXS) measurements were performed in Beamline 11-3 at the Stanford Synchrotron Radiation Lightsource (SSRL). The X-ray wavelength for the measurements was 0.973 Å. The sample to detector distance was set at 315 mm. The exposure time for each measurement was 10 s. Data were collected at an incidence angle of 0.14°, which is above the critical angle of Alq3 and therefore representative of the bulk structure of the thin film. A "χ correction"[31] was applied to the raw diffraction patterns to produce the images in Figure 1 and for the subsequent analysis in Figures 2–4. For all our analysis, we define χ to be 0° along Q_z and 90° along Q_{xy}. To produce the plots in Figures 2 and 3, intensity from χ of 10 to 85° was

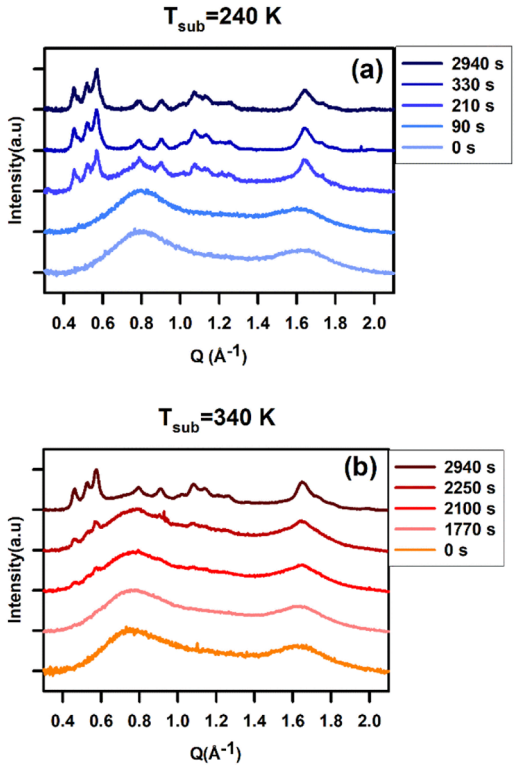

Figure 2. X-ray scattering profiles for Alq3 glasses deposited at 240 (a) and 340 K (b) at various annealing times. The Alq3 glass deposited at 240 K and annealed (at 453 K) for 210 s is clearly far more crystalline than the glass deposited at 340 K and annealed for 2100 s (at 453 K). Thus, the glass deposited at 340 K is at least ten times more resistant toward crystallization than the glass deposited at 240 K.

summed; a linear background subtraction was performed to the raw $I(Q)$ versus Q profiles subsequently.

The degree of crystallinity is determined by calculating the area under the crystalline peaks relative to the total scattered area. The degree of crystallinity is expressed mathematically as

$$\text{degree of crystallinity} = \frac{\text{total area} - \text{amorphous area}}{\text{total area}} = \frac{\text{area under crystalline peaks}}{\text{total area}} \quad (1)$$

The calculation of degree of crystallinity is outlined in detail in the Supporting Information (see Figures S6 and S7). To

https://dx.doi.org/10.1021/acs.jpcb.0c09925
J. Phys. Chem. B 2021, 125, 461–466

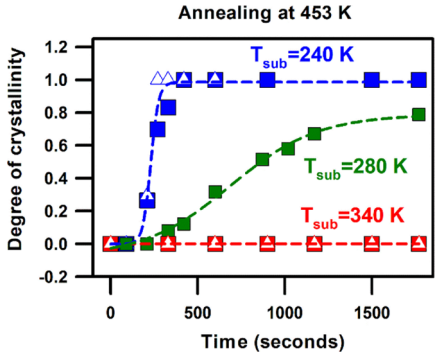

Figure 3. Degree of crystallinity as a function of annealing time for Alq3 glasses deposited at 240 K (blue symbols), 280 K (green symbols), and 340 K (red symbols). While the Alq3 glass deposited at 240 K ($0.54T_g$) finishes crystallizing by ∼420 s, the glass deposited at 340 K ($0.76T_g$) shows no evidence of crystallization for up to ∼1800 s of annealing. The glass deposited at 280 K ($0.63T_g$) crystallizes at a rate that is intermediate between the other two glasses. Filled and empty symbols represent measurements from duplicate samples, while the dashed lines are guides to the eye. The samples are annealed at 453 K ($1.01T_g$).

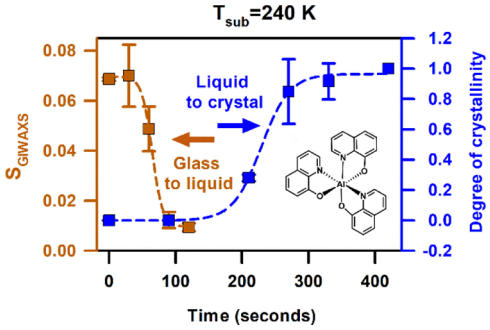

Figure 4. Hermans order parameter, S_{GIWAXS} (brown symbols) and the degree of crystallinity (blue symbols) as a function of annealing time for Alq3 glass deposited at 240 K. S_{GIWAXS} quantifies the extent of scattering anisotropy at ≈0.8 Å^{-1} and can be used to monitor the transformation of an anisotropic vapor-deposited glass into the isotropic supercooled liquid. The Alq3 glass deposited at 240 K transforms into a supercooled liquid by 90 s and crystallizes immediately afterward. Error bars are the standard deviation from measurements on two samples, and the dashed lines are eye-guides. The molecular structure of Alq3 is shown in the inset. The samples are annealed at 453 K ($1.01T_g$).

quantify the uncertainty in the degree of crystallinity, as calculated above, we compare it with an alternate method in Section SVI of the Supporting Information. The agreement between the two different methods is good.

To quantify scattering anisotropy (used below to monitor the transformation of the as-deposited glass into the supercooled liquid), we utilize the Hermans order parameter, S_{GIWAXS}.[32] The angular distribution of scattered intensity is used to compute the order parameter using the equations

$$S_{GIWAXS} = \frac{1}{2}(3\langle\cos^2\chi\rangle - 1) \quad (2)$$

where

$$\langle\cos^2\chi\rangle = \frac{\int_0^{90} I(\chi)(\cos^2\chi)(\sin\chi)\,d\chi}{\int_0^{90} I(\chi)(\sin\chi)\,d\chi} \quad (3)$$

Equation 2 has the mathematical form typical of order parameters based on the second order Legendre polynomial. Equation 3 incorporates the sine correction which is required for quantitative assessment of scattering anisotropy in 2D GIWAXS measurements.[33] The following steps were performed to calculate the order parameter: (1) for a sample produced at each deposition temperature, the peak position for the layering feature near 0.8 Å^{-1} was evaluated. (2) Data was summed from Q of 0.75 to 0.85, 0.73 to 0.83 , and 0.71 to 0.81 Å^{-1} for the glasses deposited at 240, 280, and 340 K, respectively. The integration slice was chosen such that the peak center is at the middle of the slice. (3) The $I(\chi)$ versus χ plot, obtained in step 2, was fit to a polynomial and extrapolated to fill in the data in the missing angles. (4) Data from Q of 2.17 to 2.27 Å^{-1} was used to evaluate the background and subtract the curve obtained in step 3. (5) The background subtracted $I(\chi)$ versus χ curve was used to evaluate S_{GIWAXS} (Hermans order parameter) using eqs 2 and 3.

RESULTS AND DISCUSSION

To understand the influence of deposition temperature on crystallization kinetics, we perform in situ GIWAXS on Alq3 glasses prepared at different deposition temperatures. We study films prepared at 240 K ($0.54T_g$) and 340 K ($0.76T_g$), as these deposition temperatures are expected to yield glasses with low and high kinetic stability, respectively.[34] The films are annealed at 453 K, which is ≈5 K above the reported glass transition temperature of Alq3.[35] Figure 1 shows GIWAXS patterns collected at various annealing times for Alq3 glasses deposited at 240 (a−d) and 340 K (e−h). In a GIWAXS pattern, Q_z and Q_{xy} are the out of plane and in-plane scattering vectors, respectively.[36] The colors represent intensity, as shown by the scale bar in Figure 1. Both the as-deposited glasses (T_{sub} = 240 and 340 K, t = 0 s) in Figure 1 exhibit broad scattering features at ≈0.8 and ≈1.6 Å^{-1}; such broad features are characteristic of amorphous materials. After 210 s of annealing, the diffraction pattern from the glass deposited at 240 K exhibits several sharp rings, which is characteristic of polycrystalline materials. On the other hand, the Alq3 glass deposited at 340 K is largely amorphous even after 2610 s of annealing. Figure 1 provides direct qualitative evidence that an Alq3 glass deposited at 240 K crystallizes at least ten times faster than a film deposited at 340 K. (A representative time−temperature profile for these measurements is shown in Figure S2.)

To assess the onset and progress of crystallization in PVD glasses of Alq3, we evaluate the 1D scattering plots shown in Figure 2. These 1D plots are obtained by summing intensity over the azimuthal angle in a 2D GIWAXS pattern. Figure 2 shows 1D plots for Alq3 films deposited at 240 and 340 K, at various annealing times. The t = 0 s pattern in Figure 2 shows that the as-deposited glasses of both the T_{sub} = 240 K and T_{sub} = 340 K films are fully amorphous; thus, PVD glasses of Alq3 only crystallize upon annealing after deposition. Figure 2a shows that there is a lag period of 90 s for the T_{sub} = 240 K sample, after which it crystallizes. After 330 s of annealing, crystallization is nearly complete in this sample; there is no significant evolution in the diffraction pattern after this time. The glass prepared at 340 K crystallizes much more slowly. Small sharp crystalline features between 0.4 and 0.65 Å^{-1} are visible in the t = 2100 s pattern and not in the t = 1770 s pattern. The onset time for crystallization in the T_{sub} = 340 K sample (roughly 2000 s) is an order of magnitude larger than the crystallization onset time for the glass deposited at 240 K.

https://dx.doi.org/10.1021/acs.jpcb.0c09925
J. Phys. Chem. B 2021, 125, 461−466

After a prolonged annealing time, even the T_{sub} = 340 K sample crystallizes significantly, as evident from the t = 2940 s pattern in Figure 2B. It can be seen in Figure 2 that both T_{sub} = 240 K and T_{sub} = 340 K eventually form the same polymorph upon annealing. Consistent with previous studies,[37] we find that the alpha polymorph forms upon annealing above T_g (see Figure S5).

We now turn our attention to quantitatively evaluating crystallization kinetics. Shown in Figure 3 is the degree of crystallinity as a function of annealing time. Figure 3 shows that while the Alq3 glass deposited at 240 K finishes crystallizing by ∼420 s, the T_{sub} = 340 K glass shows no evidence of crystallinity even after 1800 s of annealing. The glass deposited at 280 K crystallizes at an intermediate rate. The degree of crystallinity is mathematically defined in the methods section; a detailed discussion of this procedure can be found in Section SV of the Supporting Information.

To understand the mechanism of crystallization in PVD glasses of Alq3, we study the structure of the films before the onset of crystallization. All the as-deposited glasses of Alq3 prepared for this study exhibit a broad peak along Q_z at ≈0.8 Å^{-1}; this anisotropic scattering feature arises from a tendency toward molecular layering[38] and can be observed in Figure 1 (panels a and e). When a PVD glass transforms into a supercooled liquid, the scattering becomes isotropic.[17,39] The extent of anisotropic scattering can therefore be used to monitor the transformation of a PVD glass into a supercooled liquid. To quantify the extent of anisotropic scattering at ≈0.8 Å^{-1}, we use the Hermans order parameter, S_{GIWAXS}, defined mathematically in eqs 2 and 3 (see Methods). When S_{GIWAXS} = 1, all the scattered intensity is localized along Q_z, while a S_{GIWAXS} = −0.5 indicates that all the intensity is concentrated along Q_{xy}. Isotropic packing gives rise to a S_{GIWAXS} = 0. Figure 4 shows the S_{GIWAXS} order parameter for an Alq3 glass deposited at 240 K as a function of annealing time, as well as the crystallinity. The as-deposited glass of Alq3 exhibits a S_{GIWAXS} ≈ 0.07. However, after 90 s of annealing, this quantity becomes approximately zero, indicating that the glass has transformed into the isotropic supercooled liquid by this time. The time required for a PVD glass to transform into a supercooled liquid is a measure of its kinetic stability and depends on the deposition temperature.[17,40] While a PVD glass of Alq3 deposited at 240 K transforms into a supercooled liquid by 90 s, as shown in Figure 4, the glass deposited at 340 K shows no evidence of melting into the supercooled liquid for at least ∼2000 s (Figure S3).

It can be seen from Figure 4 that crystallization of a PVD glass of Alq3 follows a two-step process whereby it first transforms into a supercooled liquid and then crystallizes. The glass deposited at 240 K has completed melting into a supercooled liquid before any crystallization takes place, making it easy to simultaneously track glass melting and crystallization. One can envision a different scenario in more kinetically stable glasses where the parts of the glass that transform into a liquid crystallize, even while the rest of the glass is untransformed. Based on the data in Figures S3 and S4, we expect this mechanism is applicable to the glasses deposited at 340 and 280 K. Assessing the structural anisotropy in glasses that have partially crystallized is complicated due to peak overlap, making it difficult to simultaneously monitor glass melting and crystallization. However, from the data in Figures 4, S3, and S4, it is clear that the glass melting kinetics is fastest in the T_{sub} = 240 K glass and slowest in the T_{sub} = 340 K glass, with the T_{sub} = 280 K being intermediate between the two. This is the same trend seen for crystallization kinetics in Figure 3. Thus, we conclude that the glass deposited at 340 K crystallizes the slowest because it takes the longest time to transform into a supercooled liquid.

Engineering the properties of vapor-deposited glasses to modulate crystallization is an exciting new frontier in glass science and one that has important implications for technological applications. It has been shown for vanadia (VO_2)[41] and organic semiconductor CBP[11] (4,4′-bis(*N*-carbazolyl)-1,1′-biphenyl) that the structure of a vapor-deposited glass can influence which polymorph (or how much of a given polymorph) forms upon annealing. Our study demonstrates that the crystallization kinetics can also be significantly modulated by varying the glass preparation conditions. While Rodríguez-Viejo and co-workers reported a 30% slower crystallization rate in stable glasses of celecoxib compared to the liquid-cooled glass,[27] we observe an order of magnitude difference in crystallization kinetics (in glasses of varying kinetic stability). As Rodríguez-Viejo and co-workers studied crystallization below the glass transition temperature, T_g, they observe a solid (glass) → solid (crystal) transition. In this study, crystallization is observed above T_g, and consequently, we observe a solid (glass) → liquid → solid (crystal) transition. While the annealing temperature relative to T_g is relevant for comparing celecoxib and Alq3, we expect that the more important factor is that celecoxib crystallization was limited to the glass surface; for our experiments on Alq3, bulk crystal growth must occur as the entire glass sample crystallizes by the end of the experiment.

We expect the strategy of using kinetic stability to delay crystallization to be broadly applicable to organic glass-formers including those important for technological applications such as organic semiconductors. As explained in the introduction, kinetic stability characterizes the resistance of a glass toward melting into a supercooled liquid. Kinetic stability of vapor-deposited glasses has been extensively studied, and stable glasses of more than 30 organic molecules have been identified,[42] including several organic semiconductors.[7,43] Enhanced kinetic stability has already been shown to lead to higher crystallization temperatures in inorganic glass formers, such as chalcogenide[44] and metallic glasses.[45] This strategy of using kinetic stability to delay crystallization will be useful for the subset of glass-formers where crystal nucleation happens at a much faster rate than glass melting, making the latter the rate-determining step.

Our findings are also relevant to applications where an initial amorphous phase is used as a precursor to a desired crystalline phase. For these applications, a faster crystallization rate is desirable. Common preparation routes for thin films of crystalline phases of organic semiconductors like rubrene[46] and contorted hexabenzocoronene[47] involve post-deposition annealing of PVD glasses. Recently, Holmes and co-workers identified a strategy to form highly periodic patterns of organic semiconductors by crystallization of the as-deposited molecular glasses.[48] In solid-state epitaxy of complex oxides, an amorphous precursor phase is deposited on a single crystal template, which guides the crystallization process upon annealing.[49,50] For all these applications, it is likely that a faster crystallization rate can be achieved by depositing PVD glasses at temperatures that produce low stability glasses.

https://dx.doi.org/10.1021/acs.jpcb.0c09925
J. Phys. Chem. B 2021, 125, 461−466

CONCLUSIONS

We demonstrate that deposition temperature significantly influences crystallization kinetics in PVD glasses of the model organic semiconductor Alq3. Our study shows that an Alq3 glass deposited at T_{sub} = 240 K crystallizes at least ten times faster than the one prepared at T_{sub} = 340 K. This difference in crystallization kinetics is shown to be a result of the longer time taken by the more kinetically stable glass to transform into the supercooled liquid, which is an intermediate in the crystallization process. We expect our findings will be useful for the broad range of organic electronics applications which require either the inhibition or the acceleration of crystallization of molecular glasses.

ASSOCIATED CONTENT

Supporting Information

The Supporting Information is available free of charge at https://pubs.acs.org/doi/10.1021/acs.jpcb.0c09925.

GIWAXS patterns for the glass deposited at 280 K, representative time−temperature profile for the measurements shown in the study, S_{GIWAXS} as a function of annealing time for the glasses deposited at 340 and 280 K, respectively, comparison of the scattering from an annealed film of Alq3 observed in this study with the reported scattering pattern for the alpha polymorph of Alq3, description on the method of calculation of degree of crystallinity, and comparison of two different methods of calculating degree of crystallinity (PDF)

AUTHOR INFORMATION

Corresponding Author

M. D. Ediger − *Department of Chemistry, University of Wisconsin−Madison, Madison, Wisconsin 53706, United States;* orcid.org/0000-0003-4715-8473; Email: ediger@chem.wisc.edu

Authors

Kushal Bagchi − *Department of Chemistry, University of Wisconsin−Madison, Madison, Wisconsin 53706, United States;* orcid.org/0000-0002-9145-554X

Marie E. Fiori − *Department of Chemistry, University of Wisconsin−Madison, Madison, Wisconsin 53706, United States*

Camille Bishop − *Department of Chemistry, University of Wisconsin−Madison, Madison, Wisconsin 53706, United States;* orcid.org/0000-0002-2889-1752

M. F. Toney − *SLAC National Accelerator Laboratory, Stanford Synchrotron Radiation Lightsource, Menlo Park, California 94025, United States; Department of Chemical and Biological Engineering, University of Colorado Boulder, Boulder, Colorado 80309, United States;* orcid.org/0000-0002-7513-1166

Complete contact information is available at: https://pubs.acs.org/10.1021/acs.jpcb.0c09925

Notes

The authors declare no competing financial interest.

ACKNOWLEDGMENTS

We acknowledge financial support from the US Department of Energy, Office of Basic Energy Sciences, Division of Materials Sciences and Engineering, award DE-SC0002161. Data associated with this publication can be found at: https://minds.wisconsin.edu/handle/1793/75172. We thank Yuhui Li for helpful conversations.

REFERENCES

(1) Debenedetti, P. G.; Stillinger, F. H. Supercooled Liquids and the Glass Transition. *Nature* **2001**, *410*, 259−267.

(2) Angell, C. A. Formation of Glasses from Liquids and Biopolymers. *Science* **1995**, *267*, 1924−1935.

(3) Ediger, M. D.; Harrowell, P. Perspective: Supercooled Liquids and Glasses. *J. Chem. Phys.* **2012**, *137*, 080901.

(4) Telford, M. The Case for Bulk Metallic Glass. *Mater. Today* **2004**, *7*, 36−43.

(5) Yokoyama, D. Molecular Orientation in Small-Molecule Organic Light-Emitting Diodes. *J. Mater. Chem.* **2011**, *21*, 19187−19202.

(6) Ràfols-Ribé, J.; Will, P.-A.; Hänisch, C.; Gonzalez-Silveira, M.; Lenk, S.; Rodríguez-Viejo, J.; Reineke, S. High-Performance Organic Light-Emitting Diodes Comprising Ultrastable Glass Layers. *Sci. Adv.* **2018**, *4*, No. eaar8332.

(7) Bagchi, K.; Ediger, M. D. Controlling Structure and Properties of Vapor-Deposited Glasses of Organic Semiconductors: Recent Advances and Challenges. *J. Phys. Chem. Lett.* **2020**, *11*, 6935−6945.

(8) Yu, L. Amorphous Pharmaceutical Solids: Preparation, Characterization and Stabilization. *Adv. Drug Delivery Rev.* **2001**, *48*, 27−42.

(9) Lubchenko, V.; Wolynes, P. G. Photon Activation of Glassy Dynamics: A Mechanism for Photoinduced Fluidization, Aging, and Information Storage in Amorphous Materials. *J. Phys. Chem. B* **2020**, *124*, 8434−8453.

(10) Hodge, I. M. Physical Aging in Polymer Glasses. *Science* **1995**, *267*, 1945−1947.

(11) Van den Brande, N.; Gujral, A.; Huang, C.; Bagchi, K.; Hofstetter, H.; Yu, L.; Ediger, M. D. Glass Structure Controls Crystal Polymorph Selection in Vapor-Deposited Films of 4, 4′-Bis (N-Carbazolyl)-1,1′-Biphenyl. *Cryst. Growth Des.* **2018**, *18*, 5800−5807.

(12) Powell, C. T.; Xi, H.; Sun, Y.; Gunn, E.; Chen, Y.; Ediger, M. D.; Yu, L. Fast Crystal Growth in O-Terphenyl Glasses: A Possible Role for Fracture and Surface Mobility. *J. Phys. Chem. B* **2015**, *119*, 10124−10130.

(13) Esaki, Y.; Komino, T.; Matsushima, T.; Adachi, C. Enhanced Electrical Properties and Air Stability of Amorphous Organic Thin Films by Engineering Film Density. *J. Phys. Chem. Lett.* **2017**, *8*, 5891−5897.

(14) Raegen, A. N.; Yin, J.; Zhou, Q.; Forrest, J. A. Ultrastable Monodisperse Polymer Glass Formed by Physical Vapour Deposition. *Nat. Mater.* **2020**, *19*, 1110−1113.

(15) Zhang, A.; Jin, Y.; Liu, T.; Stephens, R. B.; Fakhraai, Z. Polyamorphism of Vapor-Deposited Amorphous Selenium in Response to Light. *Proc. Natl. Acad. Sci. U.S.A.* **2020**, *117*, 24076−24081.

(16) Leon-Gutierrez, E.; Sepúlveda, A.; Garcia, G.; Clavaguera-Mora, M. T.; Rodríguez-Viejo, J. Stability of Thin Film Glasses of Toluene and Ethylbenzene Formed by Vapor Deposition: An in Situ Nanocalorimetric Study. *Phys. Chem. Chem. Phys.* **2010**, *12*, 14693−14698.

(17) Dawson, K. J.; Zhu, L.; Yu, L.; Ediger, M. D. Anisotropic Structure and Transformation Kinetics of Vapor-Deposited Indomethacin Glasses. *J. Phys. Chem. B* **2011**, *115*, 455−463.

(18) Bishop, C.; Gujral, A.; Toney, M. F.; Yu, L.; Ediger, M. D. Vapor-Deposited Glass Structure Determined by Deposition Rate-Substrate Temperature Superposition Principle. *J. Phys. Chem. Lett.* **2019**, *10*, 3536−3542.

(19) Fakhraai, Z.; Still, T.; Fytas, G.; Ediger, M. D. Structural Variations of an Organic Glassformer Vapor-Deposited onto a Temperature Gradient Stage. *J. Phys. Chem. Lett.* **2011**, *2*, 423−427.

(20) Whitaker, K. R.; Tylinski, M.; Ahrenberg, M.; Schick, C.; Ediger, M. D. Kinetic Stability and Heat Capacity of Vapor-Deposited Glasses of o-Terphenyl. *J. Chem. Phys.* **2015**, *143*, 084511.

(21) Qiu, Y.; Antony, L. W.; de Pablo, J. J.; Ediger, M. D. Photostability Can Be Significantly Modulated by Molecular Packing in Glasses. *J. Am. Chem. Soc.* **2016**, *138*, 11282−11289.
(22) Qiu, Y.; Antony, L. W.; Torkelson, J. M.; de Pablo, J. J.; Ediger, M. D. Tenfold Increase in the Photostability of an Azobenzene Guest in Vapor-Deposited Glass Mixtures. *J. Chem. Phys.* **2018**, *149*, 204503.
(23) Qiu, Y.; Bieser, M. E.; Ediger, M. D. Dense Glass Packing Can Slow Reactions with an Atmospheric Gas. *J. Phys. Chem. B* **2019**, *123*, 10124−10130.
(24) Dawson, K. J.; Kearns, K. L.; Ediger, M. D.; Sacchetti, M. J.; Zografi, G. D. Highly Stable Indomethacin Glasses Resist Uptake of Water Vapor. *J. Phys. Chem. B* **2009**, *113*, 2422−2427.
(25) Smith, P. F.; Gerroir, P.; Xie, S.; Hor, A. M.; Popovic, Z.; Hair, M. L. Degradation of Organic Electroluminescent Devices. Evidence for the Occurrence of Spherulitic Crystallization in the Hole Transport Layer. *Langmuir* **1998**, *14*, 5946−5950.
(26) Aziz, H.; Popovic, Z.; Xie, S.; Hor, A.-M.; Hu, N.-X.; Tripp, C.; Xu, G. Humidity-Induced Crystallization of Tris (8-Hydroxyquinoline) Aluminum Layers in Organic Light-Emitting Devices. *Appl. Phys. Lett.* **1998**, *72*, 756−758.
(27) Rodríguez-Tinoco, C.; Gonzalez-Silveira, M.; Ràfols-Ribé, J.; Garcia, G.; Rodríguez-Viejo, J. Highly Stable Glasses of Celecoxib: Influence on Thermo-Kinetic Properties , Microstructure and Response towards Crystal Growth. *J. Non-Cryst. Solids* **2015**, *407*, 256−261.
(28) Tang, C. W.; VanSlyke, S. A. Organic Electroluminescent Diodes. *Appl. Phys. Lett.* **1987**, *51*, 913−915.
(29) Kozlov, V. G.; Bulović, V.; Burrows, P. E.; Forrest, S. R. Laser Action in Organic Semiconductor Waveguide and Double-Heterostructure Devices. *Nature* **1997**, *389*, 362−364.
(30) Dediu, V. A.; Hueso, L. E.; Bergenti, I.; Taliani, C. Spin Routes in Organic Semiconductors. *Nat. Mater.* **2009**, *8*, 707−716.
(31) Baker, J. L.; Jimison, L. H.; Mannsfeld, S.; Volkman, S.; Yin, S.; Subramanian, V.; Salleo, A.; Alivisatos, A. P.; Toney, M. F. Quantification of Thin Film Crystallographic Orientation Using X-Ray Diffraction with an Area Detector. *Langmuir* **2010**, *26*, 9146−9151.
(32) Bagchi, K.; Gujral, A.; Toney, M. F.; Ediger, M. D. Generic Packing Motifs in Vapor-Deposited Glasses of Organic Semiconductors. *Soft Matter* **2019**, *15*, 7590−7595.
(33) Hammond, M. R.; Kline, R. J.; Herzing, A. A.; Richter, L. J.; Germack, D. S.; Ro, H.-W.; Soles, C. L.; Fischer, D. A.; Xu, T.; Yu, L.; et al. Molecular Order in High-Efficiency Polymer/Fullerene Bulk Heterojunction Solar Cells. *ACS Nano* **2011**, *5*, 8248−8257.
(34) Whitaker, K. R.; Tylinski, M.; Ahrenberg, M.; Schick, C.; Ediger, M. D. Kinetic Stability and Heat Capacity of Vapor-Deposited Glasses of o-Terphenyl. *J. Chem. Phys.* **2015**, *143*, 084511.
(35) Naito, K.; Miura, A. Molecular Design for Nonpolymeric Organic Dye Glasses with Thermal Stability: Relations between Thermodynamic Parameters and Amorphous Properties. *J. Phys. Chem.* **1993**, *97*, 6240−6248.
(36) Rivnay, J.; Mannsfeld, S. C. B.; Miller, C. E.; Salleo, A.; Toney, M. F. Quantitative Determination of Organic Semiconductor Microstructure from the Molecular to Device Scale. *Chem. Rev.* **2012**, *112*, 5488−5519.
(37) Cho, C.-P.; Tu, C.-Y.; Perng, T.-P. Growth of AlQ3 Nanowires Directly from Amorphous Thin Film and Nanoparticles. *Nanotechnology* **2006**, *17*, 5506.
(38) Bagchi, K.; Jackson, N. E.; Gujral, A.; Huang, C.; Toney, M. F.; Yu, L.; de Pablo, J. J.; Ediger, M. D. Origin of Anisotropic Molecular Packing in Vapor-Deposited Alq3 Glasses. *J. Phys. Chem. Lett.* **2018**, *10*, 164−170.
(39) Bishop, C.; Thelen, J. L.; Gann, E.; Toney, M. F.; Yu, L.; DeLongchamp, D. M.; Ediger, M. D. Vapor Deposition of a Nonmesogen Prepares Highly Structured Organic Glasses. *Proc. Natl. Acad. Sci. U.S.A.* **2019**, *116*, 21421−21426.
(40) Walters, D. M.; Richert, R.; Ediger, M. D. Thermal Stability of Vapor-Deposited Stable Glasses of an Organic Semiconductor. *J. Chem. Phys.* **2015**, *142*, 134504.
(41) Stone, K. H.; Schelhas, L. T.; Garten, L. M.; Shyam, B.; Mehta, A.; Ndione, P. F.; Ginley, D. S.; Toney, M. F. Influence of Amorphous Structure on Polymorphism in Vanadia. *APL Mater.* **2016**, *4*, 076103.
(42) Ediger, M. D. Perspective: Highly Stable Vapor-Deposited Glasses. *J. Chem. Phys.* **2017**, *147*, 210901.
(43) Walters, D. M.; Antony, L.; de Pablo, J. J.; Ediger, M. D. Influence of Molecular Shape on the Thermal Stability and Molecular Orientation of Vapor-Deposited Organic Semiconductors. *J. Phys. Chem. Lett.* **2017**, *8*, 3380−3386.
(44) Zhang, K.; Li, Y.; Huang, Q.; Wang, B.; Zheng, X.; Ren, Y.; Yang, W. Ultrastable Amorphous Sb2Se3 Film. *J. Phys. Chem. B* **2017**, *121*, 8188−8194.
(45) Luo, P.; Cao, C. R.; Zhu, F.; Lv, Y. M.; Liu, Y. H.; Wen, P.; Bai, H. Y.; Vaughan, G.; Di Michiel, M.; Ruta, B.; et al. Ultrastable Metallic Glasses Formed on Cold Substrates. *Nat. Commun.* **2018**, *9*, 1389.
(46) Fielitz, T. R.; Holmes, R. J. Crystal Morphology and Growth in Annealed Rubrene Thin Films. *Cryst. Growth Des.* **2016**, *16*, 4720−4726.
(47) Hiszpanski, A. M.; Baur, R. M.; Kim, B.; Tremblay, N. J.; Nuckolls, C.; Woll, A. R.; Loo, Y.-L. Tuning Polymorphism and Orientation in Organic Semiconductor Thin Films via Post-Deposition Processing. *J. Am. Chem. Soc.* **2014**, *136*, 15749−15756.
(48) Bangsund, J. S.; Fielitz, T. R.; Steiner, T. J.; Shi, K.; Van Sambeek, J. R.; Clark, C. P.; Holmes, R. J. Formation of Aligned Periodic Patterns during the Crystallization of Organic Semiconductor Thin Films. *Nat. Mater.* **2019**, *18*, 725−731.
(49) Evans, P. G.; Chen, Y.; Tilka, J. A.; Babcock, S. E.; Kuech, T. F. Crystallization of Amorphous Complex Oxides: New Geometries and New Compositions via Solid Phase Epitaxy. *Curr. Opin. Solid State Mater. Sci.* **2018**, *22*, 229−242.
(50) Waduge, W. L. I.; Chen, Y.; Zuo, P.; Jayakodiarachchi, N.; Kuech, T. F.; Babcock, S. E.; Evans, P. G.; Winter, C. H. Solid-Phase Epitaxy of Perovskite High Dielectric PrAlO3 Films Grown by Atomic Layer Deposition for Use in Two-Dimensional Electronics and Memory Devices. *ACS Appl. Nano Mater.* **2019**, *2*, 7449−7458.

https://dx.doi.org/10.1021/acs.jpcb.0c09925
J. Phys. Chem. B 2021, 125, 461−466